Residual Circulations Calculated from Satellite Data: Their Relations to Observed Temperature and Ozone Distributions

by

Marvin A. Geller
Institute for Terrestrial and Planetary Atmospheres
State University of New York at Stony Brook
Stony Brook, NY

Eric R. Nash (1)
Applied Research Corporation
8201 Corporate Drive
Landover, MD

Mao Fou Wu (2) and Joan E. Rosenfield (3)
Laboratory for Atmospheres
NASA/Goddard Space Flight Center
Greenbelt. MD

(1) Under contract with NASA/Goddard Space Flight Center

(2) Deceased

(3) Universities Space Research Association
Columbia, MD

ABSTRACT

Monthly mean residual circulations were calculated from eight years of satellite data. The diabatic circulation is usually found to give a good approximation to the residual circulation, but this is not always the case. In particular, an example is shown at 60 °S and 30 mbar where the diabatic and residual circulations show very different annual variations. Correlations between the vertical component of the residual circulation and temperature and ozone were computed. They indicate that yearly variations of temperatures in the tropics are under dynamical control while at higher latitudes they are under radiative control, except during stratospheric warmings. Interannual variations in seasonal mean temperatures are shown to be under dynamical control everywhere. Correlations between seasonal means of the vertical component of the residual circulation and ozone mixing ratios are consistent with what would be expected from the ozone variations being due to differences in the ozone transport, although transport effects cannot easily be distinguished from photochemical effects above the altitude of the ozone mixing ratio peak. Finally, variations in total ozone are examined in comparison with residual circulations variations. A one to two month phase lag is seen in the annual variation in the total ozone at 60 °N with respect to the maximum downward residual motions. This phase lag is greater at 60 °N than at 60 °S. There is evidence at 60 °S of a greater downward trend in the mean zonal ozone maxima than there is in the minima. A decreasing trend in the maximum descending motion is seen to accompany the ozone trend at 60 °S.

1. Introduction

The Transformed Eulerian Mean (TEM) formulation of the equations of motion has proven to be very useful for the study of the middle atmosphere (see Andrews et al., 1987, for example). A principal reason for this is that the compensating effects of the eddy momentum and heat fluxes are not as apparent in the Eulerian formulation of the zonal mean equations of motion for the middle atmosphere as they are in the TEM formulation. Furthermore, the works of Andrews and McIntyre (1976), Dunkerton (1981), and Plumb and Mahlman (1987) suggest that the residual mean circulation (and the diabatic circulation) may be regarded as approximations to the Lagrangian advective motions projected onto the meridional plane.

This, together with the fact that residual mean circulations (or diabatic circulations) are very often used as the advective circulations in two-dimensional photochemical models of the middle atmosphere (e. g., Garcia and Solomon, 1983, Isaksen and Stordal, 1986, and Guthrie et al., 1990), has stimulated several recent papers that have presented calculations of the diabatic circulation and/or the residual mean circulation from stratospheric satellite data. For instance, Solomon et al. (1986) have computed the diabatic circulation for the seven months of LIMS (Limb Infrared Monitor of the Stratosphere) data (November 1978 to May 1979) and used these results in a simple two-dimensional photochemical model of methane and nitrous oxide to compare with SAMS (Stratosphere And Mesosphere Sounder) observations. Rosenfield et al. (1987) used SBUV (Solar Backscatter UltraViolet Instrument), SME (Solar Mesospheric Explorer), and NMC (NOAA National Meteorological Center) data to calculate net diabatic heating rates and the diabatic circulations for the months of January, April, July, and October to update the earlier work of Murgatroyd and Singleton (1961) and to use their new calculations to interpret departures of the observed state of the atmosphere from radiative equilibrium in terms of atmospheric wave activity. Gille et al. (1987) calculated the residual mean circulation using LIMS data, explicitly discussing the separate contributions to this circulation from the diabatic circulation and that due to transient wave activity. Callis et al. (1987) calculated the monthly mean values of the residual mean circulation and used these results to estimate stratospheric lifetimes of air parcels circulating in the meridional plane. They also made some preliminary estimates of the interannual variability of the diabatic circulation.

In this paper, results are shown for the calculations of the monthly mean meridional circulation from December 1978 to October 1986. The computed residual mean circulations are compared to computed diabatic circulations to illustrate some circumstances where they compare well and also where they compare poorly. Since the zonally averaged thermodynamic equation can be written in a form where the principal dynamics effects arise through the residual circulation, comparison is made between variations in the residual mean circulation and variations in temperature. This is done for both annual variations and interannual variations in temperature. This gives information on which regions of the atmosphere have temperature variations on these time scales that are predominantly under dynamic control and in which regions these temperature variations are predominantly under radiative control. Comparisons are also made between ozone variations and variations in the computed residual circulation.

2. Calculations

The data used in this paper are NOAA/NMC temperature data extending for a period of almost eight years from December 1978 to October 1986, ozone profile data from 30 to 0.4 mbar from the SBUV instrument on Nimbus 7 for this same period. Below 30 mbar, the ozone climatology that is used in the SBUV data reduction algorithm was used.

The equations defining the monthly averaged vertical and meridional components of the residual mean circulation are as follows:

$$[\bar{v}_{res}] = [\bar{v}] - \frac{1}{\rho}\frac{\partial}{\partial z}\left(\rho\left\{[\bar{v}^*\bar{\theta}^*] + [\overline{v'\theta'}]\right\} / \frac{d[\bar{\theta}]}{dz}\right) \qquad (1)$$

$$[\bar{w}_{res}] = [\bar{w}] + \frac{1}{\rho\cos\phi}\frac{\partial}{\partial y}\left(\rho\cos\phi\left\{[\bar{v}^*\bar{\theta}^*] + [\overline{v'\theta'}]\right\} / \frac{d[\bar{\theta}]}{dz}\right) \qquad (2)$$

For the most part, conventional notation is used in writing equations (1) and (2). v is the northward wind. w is the upward wind. ρ is

density. θ is potential temperature. z is the log pressure height coordinate. ϕ is latitude. y is distance measured in the northward direction from the Equator. The square brackets indicate zonal averages. The overbars indicate monthly averages. The * superscripts indicate departures from zonal averages, and the prime superscripts indicate departures from the monthly averages. Equations (1) and (2) then differ from the equations introduced by Andrews and McIntyre (1976) in that the monthly averaged eddy heat flux term consists of two parts, that due to the monthly mean standing eddies, $[\overline{v}^*\overline{\theta}^*]$ and that due to the monthly average of the transient eddies, $\overline{[v'\theta']}$. Otherwise, the terms in equations (1) and (2) have the same meaning as in Andrews and McIntyre (1976).

With the components of the residual circulation defined by equations (1) and (2), the zonal mean thermodynamic equation can be written as

$$\frac{\partial[\overline{\theta}]}{\partial t}+[\overline{v}_{res}]\frac{\partial[\overline{\theta}]}{\partial y}+[\overline{w}_{res}]\frac{\partial[\overline{\theta}]}{\partial z}=$$

$$[\overline{Q}]-\frac{1}{\rho}\frac{\partial}{\partial z}\rho\left(\left\{[\overline{v}^*\overline{\theta}^*]+\overline{[v'\theta']}\right\}\frac{\partial[\overline{\theta}]}{\partial y}\Big/\frac{\partial[\overline{\theta}]}{\partial z}+\left\{[\overline{w}^*\overline{\theta}^*]+\overline{[w'\theta']}\right\}\right) \qquad (3)$$

Equation (3) is used together with the equation of continuity,

$$\frac{\partial}{\partial y}\left([\overline{v}_{res}]\cos\phi\right)+\frac{1}{\rho}\frac{\partial\left([\overline{w}_{res}\rho]\right)}{\partial z}=0 \qquad (4)$$

to calculate the residual circulation in the following manner. The first term on the left-hand side of equation (3) is computed by centered time differencing using the monthly averaged potential temperatures. In the second term on the left-hand side of equation (3), $[\overline{v}_{res}]$ is initially taken to be zero. The eddy heat flux terms on the right-hand side of equation (3) are calculated from data. In these computations, v is computed geostrophically and w is computed using the thermodynamic equation using the radiation scheme in

Rosenfield et al. (1987) with the ozone and temperature data. $[\overline{Q}]$ is also computed using the radiation scheme in Rosenfield et al. (1987) and the ozone and temperature data. Thus, an initial estimate is obtained for $[\overline{w}_{res}]$ from equation (3). The distribution of $[\overline{w}_{res}]$ is adjusted to make

$$\int_{-90^\circ}^{+90^\circ}[\overline{w}_{res}]\cos\phi dy = 0$$

These adjusted values for $[\overline{w}_{res}]$ are put into equation (4) to obtain a revised estimate for $[\overline{v}_{res}]$. This revised estimate for $[\overline{v}_{res}]$ is used in equation (3) to obtain a revised estimate for $[\overline{w}_{res}]$, and this procedure is repeated until convergence is obtained. This is essentially the same technique that was used by Solomon et al. (1986) and Gille et al. (1987). It usually converges in about four to five iterations.

3. Results

The diabatic circulation and the residual mean circulation are commonly taken to be approximations to the transport circulation in the meridional plane in two-dimensional photochemical models. Under certain conditions, however, the diabatic and residual circulations are known to differ from one another (see Rosenfield and Schoeberl, 1986, for instance). Thus, we wish to examine the circumstances where these circulations depart from one another.

3.1 Diabatic and Residual Circulations

Figure (1) shows a comparison between the vertical components of the computed residual mean and diabatic circulations at two points in the meridional plane, 60 °N and 60 °S, both at 30 mbar. The diabatic and residual mean curves at 60° N agree well with one another, but those at 60 °S do not. In fact, the vertical components of the diabatic and residual mean circulations at 60 °S often vary out of phase with one another.

To better understand this very different relation between the diabatic and residual circulations at 60 °N and 60 °S, we start by referring back to equation (3) where the equation for the diabatic circulation is defined by the underlined terms whereas the full

equation defines the residual mean circulation. Thus, the determination of the residual mean motions from the thermodynamic equation involves both the temperature tendency term and eddy heat flux terms that do not appear in the equation for the diabatic circulation. Figure (2) shows a comparison between the temperature tendency term and the diabatic heating term in equation (3). A very different behavior is seen at 60 °S than at 60 °N. At 60 °N, the variations in the heating rate are two to three times larger than those of the temperature tendency term; that is to say, the absolute value of the temperature tendency term is always less than 0.2 °K/day whereas the heating rate term varies between +0.2 and -0.7 °K/day. The heating rate term at 60 °N varies from its maximum value in the June-July period to its minimum in the January-February time period. The effects of final stratospheric warmings are clearly seen in the temperature tendency term at 60 °N in the local maximum that is seen each year around March. At 60 °S, quite a different picture is seen in which the temperature tendency term varies out of phase from the heating term and the range of variation in these two terms are very much the same. That is to say, the temperature tendency term varies between +0.2 and -0.4 °K/day and the heating rate term varies between about -0.1 and -0.5 °K/day. In trying to see the physical reasons behind the different behavior at 60 °N and 60 °S, an obvious difference is that the larger land-sea contrasts and orography in the Northern Hemisphere gives rise to much larger large-scale wave activity in the Northern Hemisphere. These greater wave effects give a much greater driving of the winter atmosphere away from radiative equilibrium in the Northern Hemisphere.

Comparing figures (1) and (2), one sees that at 60 °N, the variations of both the diabatic and residual circulations follow closely the variations in the heating rate term, whereas at 60 °S variations in the diabatic circulation follow the heating rate term term but the residual circulation does not. Thus, the residual circulation and the diabatic circulation at 60 °N and 30 mbar are predominantly determined by local heating imbalances that result from the effects of atmospheric wave motions. At 60 °S, on the other hand, the diabatic circulation is a result of local imbalances in the heating, as must be the case from the equations for the diabatic circulation, but the temperature tendencies and the residual circulation do not

represent local responses but rather are responses to the global pattern of heating and circulation. (1) The essential The essential difference between the situation at 60 °N and 60 °S must be a consequence of the lesser atmospheric wave activity at 60 °S such that local imbalances in the heating rate are not being forced as strongly as at 60 °N.

3.2 Correlations Between $[\overline{w}_{res}]$ and $[\overline{T}]$

Equation (3) indicates that temperature variations in the atmosphere are controlled by meridional and vertical residual mean motions, by diabatic heating, and by meridional and vertical eddy heat fluxes. It is usually the case that the two most important of these effects for maintaining the global pattern of temperatures are diabatic heating and residual mean vertical motions. If it is dynamics that is maintaining the temperature variations, one should expect to see a negative correlation between $[\overline{w}_{res}]$ and $[\overline{T}]$; that is to say, downward motions lead to compressional heating and upward motions lead to expansion cooling. Figure (3) shows the correlation pattern between the departures of $[\overline{w}_{res}]$ and $[\overline{T}]$. This correlation pattern consists of a low latitude region of high negative correlation that tilts northward with increasing altitude and regions of high positive correlation poleward of this (except for a small region of negative correlation at high southern latitudes and low altitudes).

We propose the following explanation for this correlation pattern. The low latitude stratosphere is known to be under strong dynamic control by the rising branch of the Hadley circulation and its variations. It is well known that this is the reason for the existence for the high cold tropopause in this region of the atmosphere, for example. Thus, the negative correlations in the tropics indicate a causal relationship between variations in the vertical motion that are forced from below and the temperature response. The explanation for the regions of positive correlations at the high latitudes of both hemispheres is less straightforward. By and large, it is observed that

---

(1) Andrews et al. (1987) discuss how the governing equation for temperature changes takes the form of an elliptic equation. The behavior discussed above is consistent with the characteristics of elliptic equations.

the annual variation in stratospheric temperatures is under solar radiative control at these higher latitudes. For example, at these altitudes and latitudes, the temperatures are cooler in winter than in summer. As one progresses through the year from summer to winter, however, the planetary wave activity also increases. This is accompanied by increasing dynamic heating at the high latitudes of the winter hemisphere. Within the TEM formulation, this increasing dynamical heating manifests itself as an increasing downward component of the residual mean circulation at these latitudes. Thus, as the temperature decreases at middle and high latitudes, there is increasing downward mean residual circulation which results in the positive correlation that is seen at the middle and high latitudes of the stratosphere in figure (3).

It is instructive to examine time series of $[\overline{w}_{res}]$ and $[\overline{T}]$ at two points in the meridional plane, one at which the correlation is positive and the other at which the correlation is negative. These two points are indicated by the "x" marks in figure (3). The point at 0 ^{o} and 5 mbar lies in the heart of the negative correlation region, and the point at 60 ^{o}N and 10 mbar lies near the heart of the positive correlation region. These time series are shown in figure (4). At 0 ^{o} and 5 mbar, a very close tracking of these curves (-$[\overline{w}_{res}]$ and $[\overline{T}]$) is seen, illustrating that there is not only correlation in the overall annual variation but also in the details of of the variations. This is a good indication of the dynamical control of the temperature variations at all time scales. The situation is very different at 60 ^{o}N and 10 mbar. Here, one sees a general correlation between the two curves ($[\overline{w}_{res}]$ and $[\overline{T}]$), but certainly the details are not so closely correlated. In fact, during Northern Hemisphere winter of each year, there is a period during which the variations in temperature and the vertical component of the residual mean circulation are clearly anticorrelated. These are the periods of stratospheric warmings during which the temperatures are under dynamic control. These periods of dynamic control are imbedded in a background in which the temperature variations are predominantly under radiative control.

These results are reminiscent of some of the conclusions of Fels et al. (1980) who compared full general circulation modeling of the temperature response to halved ozone and doubled carbon dioxide distributions with the results of two-dimensional fixed-dynamical-heating models. One of Fels' et al. (1980) conclusions was that the

fixed-dynamical-heating model generally gave very similar results to those of the general circulation models at middle and high latitudes, and that different results were seen in the tropics. They suggested that outside the tropics the temperature response was being determined by changes in radiative heating but that the dynamical heating remained relatively unchanged (i. e., "fixed-dynamical-heating"). On the other hand, in the tropics the changes in the dynamical heating were playing a large role in determining the altered temperature distribution. This is consistent with our suggestion that the mid and high latitude stratospheric temperatures are predominantly under radiative control while the tropical stratospheric temperatures are under dynamical control.

In the previous discussion, it was argued that either dynamical or radiative processes can play the predominant role in determining the annual variation of temperature in different regions of the stratosphere. On the other hand, it is anticipated that interannual differences in the seasonal means of temperature are determined by interannual variations in dynamics. To test this hypothesis, we have computed the correlations between linearly detrended seasonal means of $[\overline{T}]$ and $[\overline{w}_{res}]$. The purpose of the detrending is to eliminate correlations due to secular changes from either instrumental or climate change considerations. Figure (5) shows the results of these calculations for the December-January-February (DJF) season (although the other seasons also show similar results). Negative correlations exist over almost the entire domain in figure (5). The shaded regions indicate where the correlation coefficient is negative. Those correlation values whose absolute values lie between 0.6 and 1.0 indicate regions where the sign of the correlation is certain with a confidence level in excess of 90%. Thus, these results suggest that the interannual variations in temperature structure are dynamically controlled.

3.3 Correlations Between $[\overline{w}_{res}]$ and O_3

The distribution of zonally averaged ozone with altitude and latitude is determined by photochemistry together with advection by the zonally-averaged transport circulation and diffusive processes (see Plumb and Mahlman, 1987). In this section, we inquire to what extent interannual variations in the computed residual mean circulation can be related to observations of the interannual variations of ozone. Figure (6) shows the correlations between the

detrended vertical component of the residual mean circulation and the ozone mixing ratio for the DJF season. These results are quite noisy, but focussing attention on the overall pattern of the correlation coefficients, one sees that mostly positive values are seen above the solid line, which indicates the level of the ozone mixing ratio peak during this season, while mostly negative values of the correlation coefficient are seen below the line. Also, in figure (6), one sees that in the stratosphere all regions in which the correlations are negative to a certainty exceeding 90% $(r \leq -0.6)$ lie below the line while the regions where the correlations are positive to a certainty exceeding 90% $(r \geq 0.6)$ lie mostly above the line. Again only one season is shown, but the other three seasons show this same pattern. This general correlation pattern is consistent with what would be produced by vertical advection; that is to say, downward motion will produce local decreases in ozone mixing ratios above the altitude of the ozone peak mixing ratio and produce local increases below, and upward vertical motions would result in the opposite. At high altitudes, one must also consider the effects of temperature-dependent photochemistry, however. Downward vertical motions, for example, would give rise to temperature increases through compressional heating and this would increase the rate of ozone loss through the temperature dependence of the chemical reaction rates. Thus, downward motion would result in ozone loss giving a positive correlation between the ozone mixing ratios and $[\overline{w}_{res}]$. Upward motion would do the opposite. Figure (7) shows the correlation pattern between ozone mixing ratio and temperatures also for the DJF season. Comparing figures (6) and (7) we see that these figures are approximately the negative of one another as must be the case given the strong negative correlations between $[\overline{w}_{res}]$ and $[\overline{T}]$ that were seen in figure (5). Thus, the positive correlations that are seen between $[\overline{w}_{res}]$ and the ozone mixing ratio above the level of peak ozone mixing ratio are in the sense implied by both vertical zone advection and by temperature-dependent photochemistry. The negative correlations below the ozone peak are in the sense that is implied by vertical ozone transport. Temperature-dependent photochemistry is not a consideration in this region due to the very long photochemical lifetime for ozone there.

3.4 $[\overline{w}_{res}]$ and Total Ozone

Finally, we wish to examine associations between $[\overline{w}_{res}]$ and total column ozone. Figure (8) shows the comparison between time series of monthly mean total ozone and $[\overline{w}_{res}]$ at 60 °N and S at 30 mbar. In figure (8), the annual cycle in total ozone is seen to be smaller at 60 °S than at 60 °N. Also, the maximum total ozone amounts are seen to occur a couple of months later with respect to the Spring Equinox at 60 °S than at 60 °N.

At 60 °N, the maximum downward residual mean motion occurs around January-February with near zero $[\overline{w}_{res}]$ occurring around June-July. The maximum downward motions are about 60 x 10^{-3} cm s^{-1} at 60 °N. At 60 °S, the maximum downward motions usually occur during September-October, but the shape of the annual variation curve for $[\overline{w}_{res}]$ is not nearly so regular at 60 °S as it is at 60 °N with a secondary maximum in downward motion often occurring during April-May. This is consistent with the annual variation of planetary waves that is discussed by Geller et al. (1989). At 60 °S, the maximum downward motions are about 40-45 x 10^{-3} cm s^{-1}. At 60 °S, the weakest vertical residual mean motions occur during June-July and are about -10-20 x 10^{-3} cm s^{-1} (except in early 1979) and occur during the first half-year. Thus, these calculations indicate that the summer Northern Hemisphere is much closer to radiative equilibrium (near zero $[\overline{w}_{res}]$) than is the summer Southern Hemisphere, or possibly there is a missing heating term that we are not considering in our calculations. It is also seen that in several of the years (1980, 1981, 1982, 1983, and 1985), two periods of weak $[\overline{w}_{res}]$ are seen at 60 °S, one in January-February and the other in July-August.

It is interesting that at 60 °S the main ozone maximum in Spring coincides with (or lags a bit behind) the main maximum in downward motion. At 60 °N, more of a phase lag is evident between the ozone maximum and the downward motion. This is consistent an ozone response to the time-integrated vertical transport. The larger phase lag at 60 °N is consistent with the vertical motion variations at 60 °N being smoother and more gradual than those at 60 °S.

Finally, it should be mentioned that the SBUV ozone data used here have not been normalized with respect to ground-based measurements, so instrumental drift effects are not corrected for, but presumedly such instrumental effects should be the same in each hemisphere. By examining the trends, if any, in the dynamics which transport ozone, one may seek to distinguish between chemical and dynamics effects. Looking first at the results at 60 ^{o}N, one sees an apparent secular decrease in the ozone minima by about 20 DU over the eight years (or about a 5% decrease) without any similar trend being seen in the vertical motions. At 60 ^{o}S, however, one sees a decrease of about 50-60 DU (about 15%) in the ozone maxima and about a 20-30 DU in the ozone minima (about 8%). At the same time, a decrease in the downward motion minima from about -45 x 10^{-3} cm s^{-1} to about 30 x 10^{-3} cm s^{-1} is seen. No obvious trend is seen in the downward motion maxima, however. Presumably, we may attribute some of this decrease in the maximum ozone amounts to the changing dynamics (see Wu at al., 1987) for example.

4. Summary

Using approximately eight years of NMC stratospheric temperature and SBUV data (December 1978 to October 1986), we have calculated the monthly mean residual circulations. Our most significant findings are as follows:

(1) Under most conditions, the diabatic circulation is a good approximation to the residual mean circulation, but under some circumstances, there is little correspondence between these two circulations. This has been shown to be the case at 60 ^{o}S and 30 mbar where the variations of the temperature tendency term are much larger than those of the diabatic heating term. Thus, at 60 ^{o}S and 30 mbar, the temperature tendency term and the residual circulation do not respond to local heating rates but rather are part of a global response.

(2) The computed correlations between variations in the monthly means of the vertical component of the residual circulation and zonal mean temperatures are negative in the tropics and positive at higher latitudes. This is interpreted to indicate that in the tropics the annual variations in the temperature are responding dynamically to vertical motions forced from below. At higher latitudes, the temperature are mainly responding to radiative forcing except during stratospheric warmings in Northern Hemisphere winter. The

correlations between variations in the seasonal averages of temperature and the vertical component of the residual mean circulation are found to be predominantly negative indicating dynamical control of the interannual variations in the seasonal averages of the temperature field.

(3) The computed correlations for variations in the seasonal mean of the vertical component of the residual mean circulation and the ozone mixing ratios show a pattern consistent with what is to be expected from vertical transport. Positive correlations are found above the ozone peak, and negative correlations are found below. The positive correlation above the peak is also in the sense expected to result from temperature-dependent ozone loss rates.

(4) A larger decreasing trend is seen in the ozone maxima at 60 ^{o}S than at 60 ^{o}N (about 50-60 DU at 60 ^{o}S versus about 20 DU at 60 ^{o}N over the eight years). No obvious trend is seen in the residual mean motions at 60 ^{o}N, but a weakening trend in the strength of the maximum descending motions is seen at 60 ^{o}S.

Acknowledgements

The authors would like to acknowledge very useful discussions on earlier versions of this manuscript with Drs. Mark Schoeberl, Richard Rood, and Jack Kaye. Much of this work has been supported by NASA Upper Atmosphere Theory Program funding to the Goddard Space Flight Center. M. A. Geller has also received support for this work from Grant NAG 5-1206 from the Goddard Space Flight Center and NAGW 2106 from NASA Headquarters.

References

Andrews, D. G., J. R. Holton, and C. B. Leovy, 1987: *Middle Atmosphere Dynamics*. Academic, 489 pp.

Andrews, D. G., and M. E. McIntyre, 1976: Planetary waves in horizontal and vertical shear: The generalized Eliassen-Palm relation in the mean zonal acceleration. *J. Atmos. Sci., 33*, 2031-2048.

Callis, L. B., R. E. Boughner, and J. D. Lambeth, 1987: The stratosphere: Climatologies of the radiative heating and cooling rates and the diabatically diagnosed net circulation fields. *J. Geophys. Res., 92*, 5585-5607.

Dunkerton, T., 1978: On the mean meridional motions of the stratosphere and mesosphere. *J. Atmos. Sci., 44*, 2325-2333.

Fels, S. B., J. D. Mahlman, M. D. Schwarzkopf, and R. W. Sinclair, 1980: Stratospheric sensitivity to perturbations in ozone and carbon dioxide: radiative and dynamic response. *J. Atmos. Sci., 37*, 2265-2297.

Garcia, R. R., and S. Solomon, 1983: A numerical model of the zonally averaged dynamical and chemical structure of the middle atmosphere. *J. Geophys. Res., 88*, 1379-1400.

Geller, M. A., M. F. Wu, and E. Nash, 1989: Satellite data analysis of ozone differences in the northern and southern hemispheres. *PAGEOPH, 130*, 263-275.

Gille, J. C., L. V. Lyjak, and A. Smith, 1987: The global residual circulation in the middle atmosphere for the northern winter period. *J. Atmos. Sci., 44*, 1437-1452.

Guthrie, P. D., C. H. Jackman, T. L. Kucsera, and J. E. Rosenfield, 1990: On the sensitivity of a residual circulation model to differences in input temperature data. *J. Geophys. Res., 95*, 873-882.

Isaksen, I. S. A., and F. Stordal, 1986: Ozone perturbations by enhanced levels of CFC's, N_2O and CH_4: A two-dimensional

diabatic circulation study including uncertainty estimates. *J. Geophys. Res.*, *91*, 5249-5263.

Murgatroyd, R. J., and F. Singleton, 1961: Possible meridional circulations in the stratosphere and mesosphere. *Quart. J. Roy. Meteor. Soc.*, *87*, 125-135.

Plumb, R. A., and J. D. Mahlman, 1987: The zonally-averaged transport characteristics of the GFDL general circulation/transport model. *J. Atmos. Sci.*, *44*, 298-327.

Rosenfield, J. E., and M. R. Schoeberl, 1986: A computation of stratospheric heating rates and the diabatic circulation for the Antarctic spring. *Geophys. Res. Lett.*, *13*, 1339-1442.

Rosenfield, J. E., M. R. Schoeberl, and M. A. Geller, 1987: A computation of the stratospheric diabatic circulation using an accurate radiative transfer model. *J. Atmos. Sci.*, *44*, 859-876.

Solomon, S., J. T. Kiehl, R. C. Garcia, and W. Grose, 1986: Tracer transport by the diabatic circulation deduced from satellite observations. *J. Atmos. Sci.*, *43*, 1603-1617.

Wu, M.-F., M. A. Geller, J. G. Olson, and E. M. Larsen, 1987: A study of global ozone transport and the role of planetary waves using satellite data. *J. Geophys. Res.*, *92*, 3081-3097.

Figure Captions

Figure 1: Top - Time series of monthly mean diabatic and residual circulations at 60 °N and 30 mbar. Bottom - Time series of monthly mean diabatic and residual circulations at 60 °S and 30 mbar. Units are 10^{-2} cm s^{-1}.

Figure 2: Top - Time series of diabatic heating term and temperature tendency term in equation (3) at 60 °N and 30 mbar. Bottom - Time series of diabatic heating term and temperature tendency term in equation (3) at 60 °S and 30 mbar. Units are °K day^{-1}.

Figure 3: Pattern of correlation between $[\overline{w}_{res}]$ and $[\overline{T}]$ as a function of altitude (24 to 55 km) and latitude (pole to pole). The shading denotes regions where the correlation coefficients are negative.

Figure 4: Top - Time series of $[\overline{T}]$ and $-[\overline{w}_{res}]$ at 0 ° and 5 mbar. Bottom - Time series of $[\overline{T}]$ and $[\overline{w}_{res}]$ at 60 °N and 10 mbar. Standard deviation units are used so that the variations of $[\overline{T}]$ and $[\overline{w}_{res}]$ may be shown on the same scale.

Figure 5: Pattern of correlation between interannual variations of December- January-February averages of $[\overline{w}_{res}]$ and $[\overline{T}]$ as a function of altitude (24 to 55 km) and latitude (pole to pole). Both $[\overline{w}_{res}]$ and $[\overline{T}]$ have been detrended in computing these correlations. The shading denotes regions where the correlation coefficients are negative. Within regions where $|r| > 0.6$, the sign of the correlation is certain with 90% confidence.

Figure 6: Pattern of correlation between interannual variations of December- January-February averages of $[\overline{w}_{res}]$ and $[\overline{O}_3]$ as a function of altitude (24 to 55 km) and latitude (pole to pole). Both $[\overline{w}_{res}]$ and $[\overline{O}_3]$ have been detrended in computing these correlations. The shading denote regions where the correlation coefficients are negative. The heavy wavy line through the middle denotes the mean position of the altitude of the peak ozone mixing ratio as a function of latitude. Within regions where $|r| > 0.6$, the sign of the correlation is certain with 90% confidence.

Figure 7: Pattern of correlation between interannual variations of December- January-February averages of $[\overline{T}]$ and $[\overline{O}_3]$ as a function of altitude (24 to 55 km) and latitude (pole to pole). Both $[\overline{T}]$ and $[\overline{O}_3]$ have been detrended in computing these correlations. The shading denotes regions where the correlation coefficients are negative.

Figure 8: Time series of monthly mean total ozone and $-[\overline{w}_{res}]$ at 30 mbar. Top shows results at 60 °N and bottom shows results at 60 °S. The units for total ozone are Dobson units, and the units for $[\overline{w}_{res}]$ are 10^{-3} cm s^{-1}.

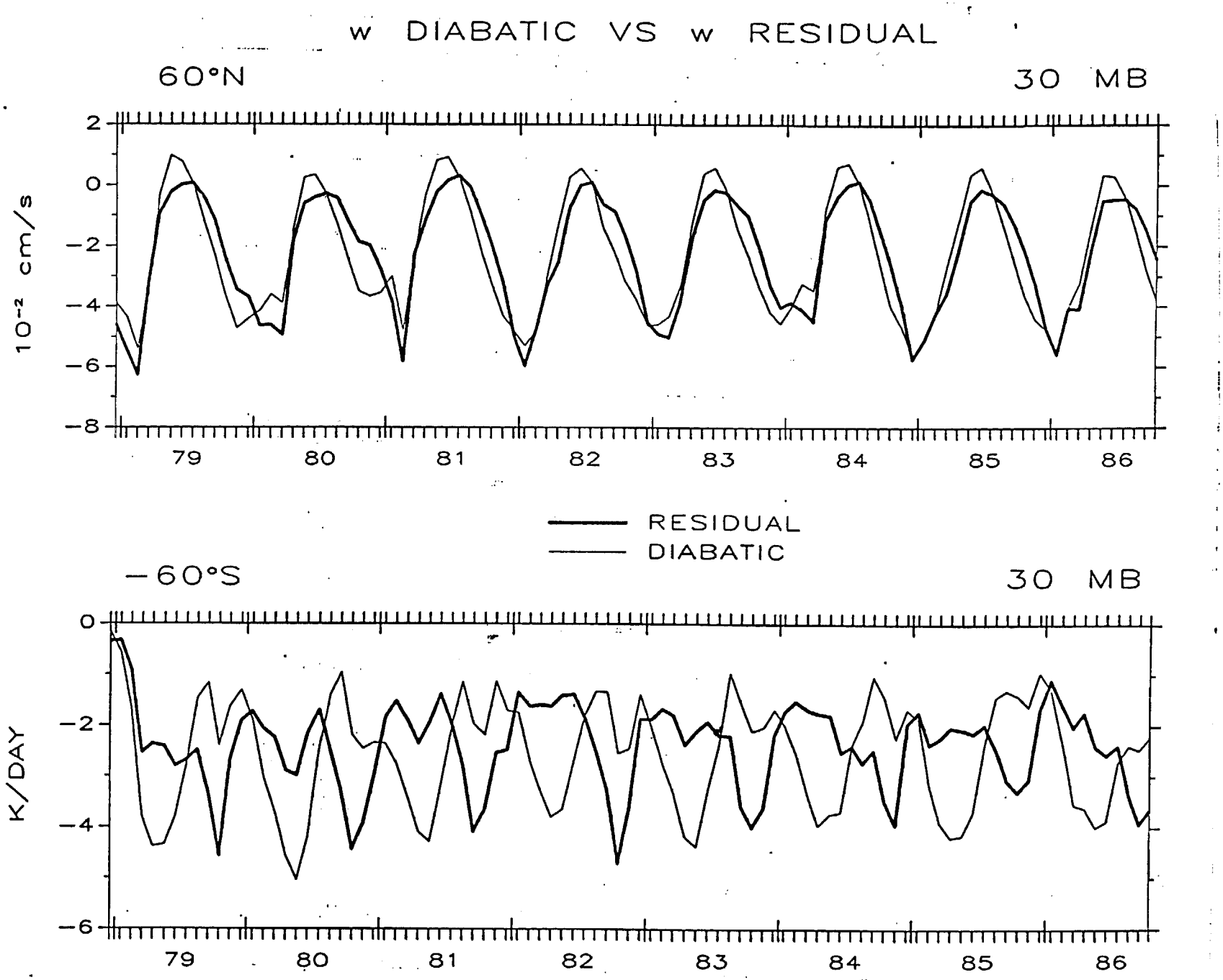
w DIABATIC VS w RESIDUAL
60°N
30 MB
10⁻² cm/s
2
0
−2
−4
−6
−8
79
80
81
82
83
84
85
86
RESIDUAL
DIABATIC
−60°S
30 MB
K/DAY
0
−2
−4
−6
79
80
81
82
83
84
85
86

F. . 1

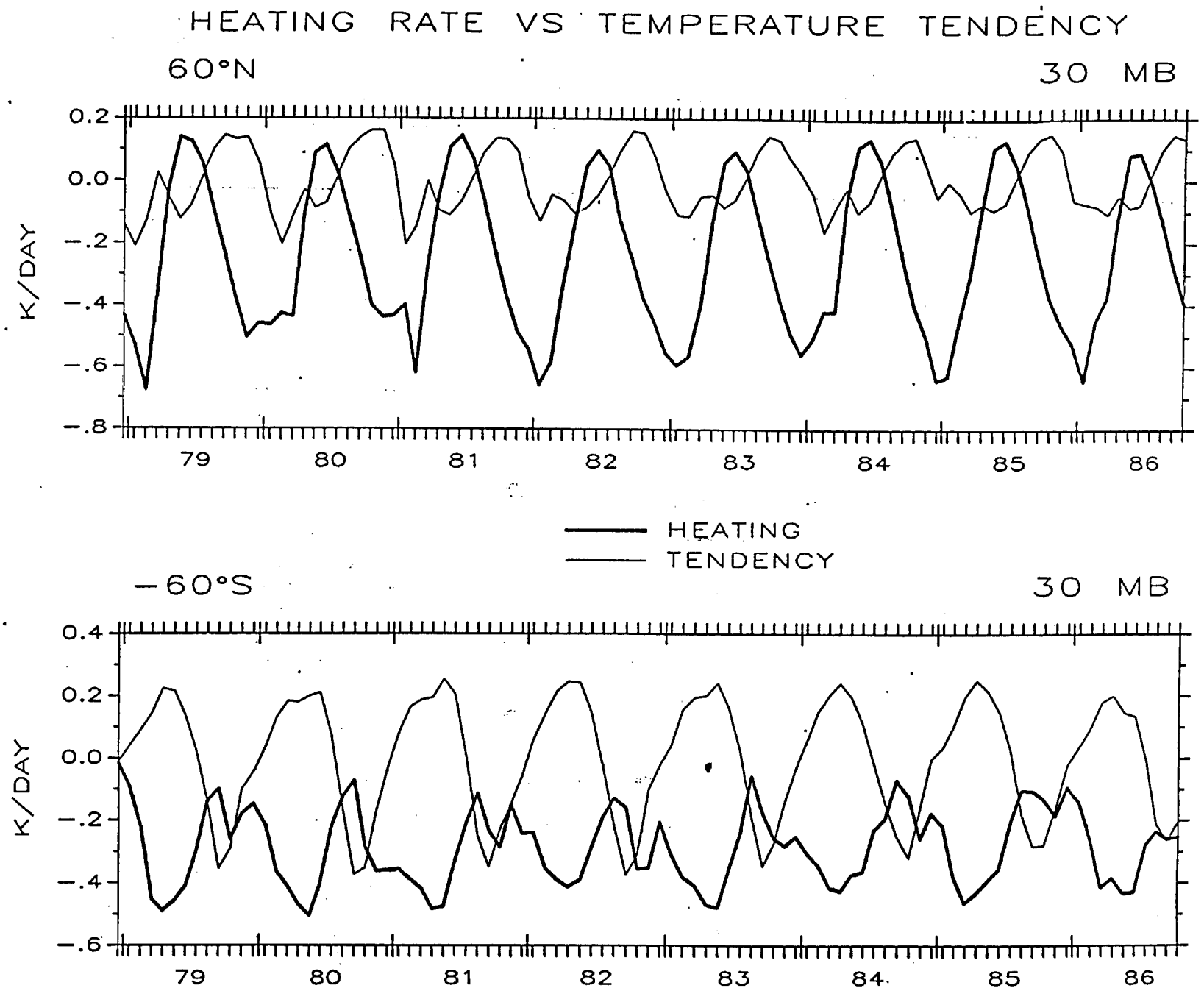
HEATING RATE VS TEMPERATURE TENDENCY
60°N
30 MB
0.2
0.0
-.2
-.4
-.6
-.8
K/DAY
79
80
81
82
83
84
85
86
HEATING
TENDENCY
-60°S
30 MB
0.4
0.2
0.0
-.2
-.4
-.6
K/DAY
79
80
81
82
83
84
85
86

Figure 2

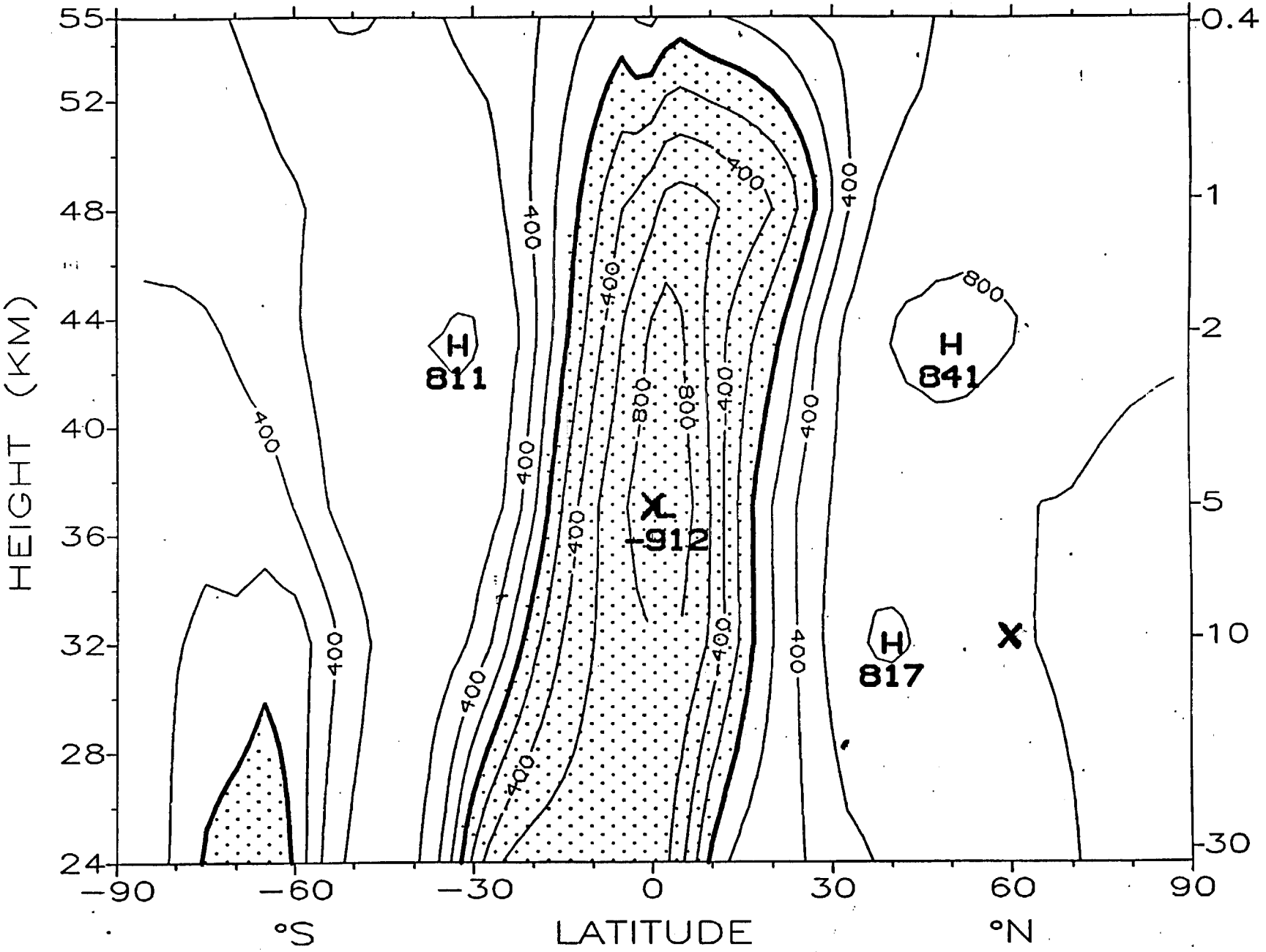
CORRELATION: W(RES) VS T
HEIGHT (KM)
55
52
48
44
40
36
32
28
24
PRESSURE (MB)
0.4
1
2
5
10
30
H
811
H
841
H
817
X
-912
X
400
800
−90
−60
−30
0
30
60
90
°S
LATITUDE
°N
CONTOUR FROM −800.00 TO 800.00 CONTOUR INTERVAL OF 200.00

F. . 7

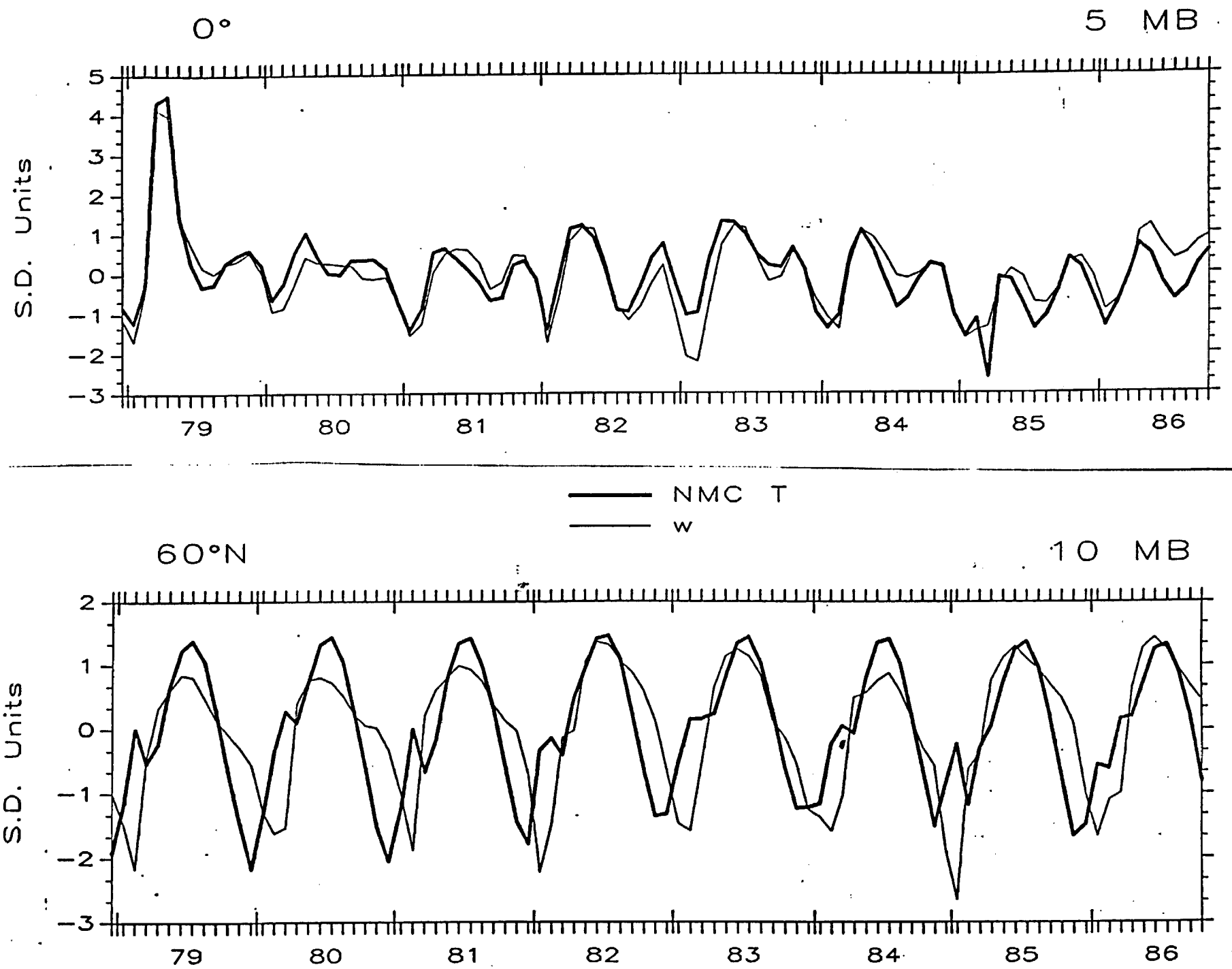
0°
5 MB
S.D. Units
5
4
3
2
1
0
−1
−2
−3
79
80
81
82
83
84
85
86
NMC T
w
60°N
10 MB
S.D. Units
2
1
0
−1
−2
−3
79
80
81
82
83
84
85
86

Figure 4

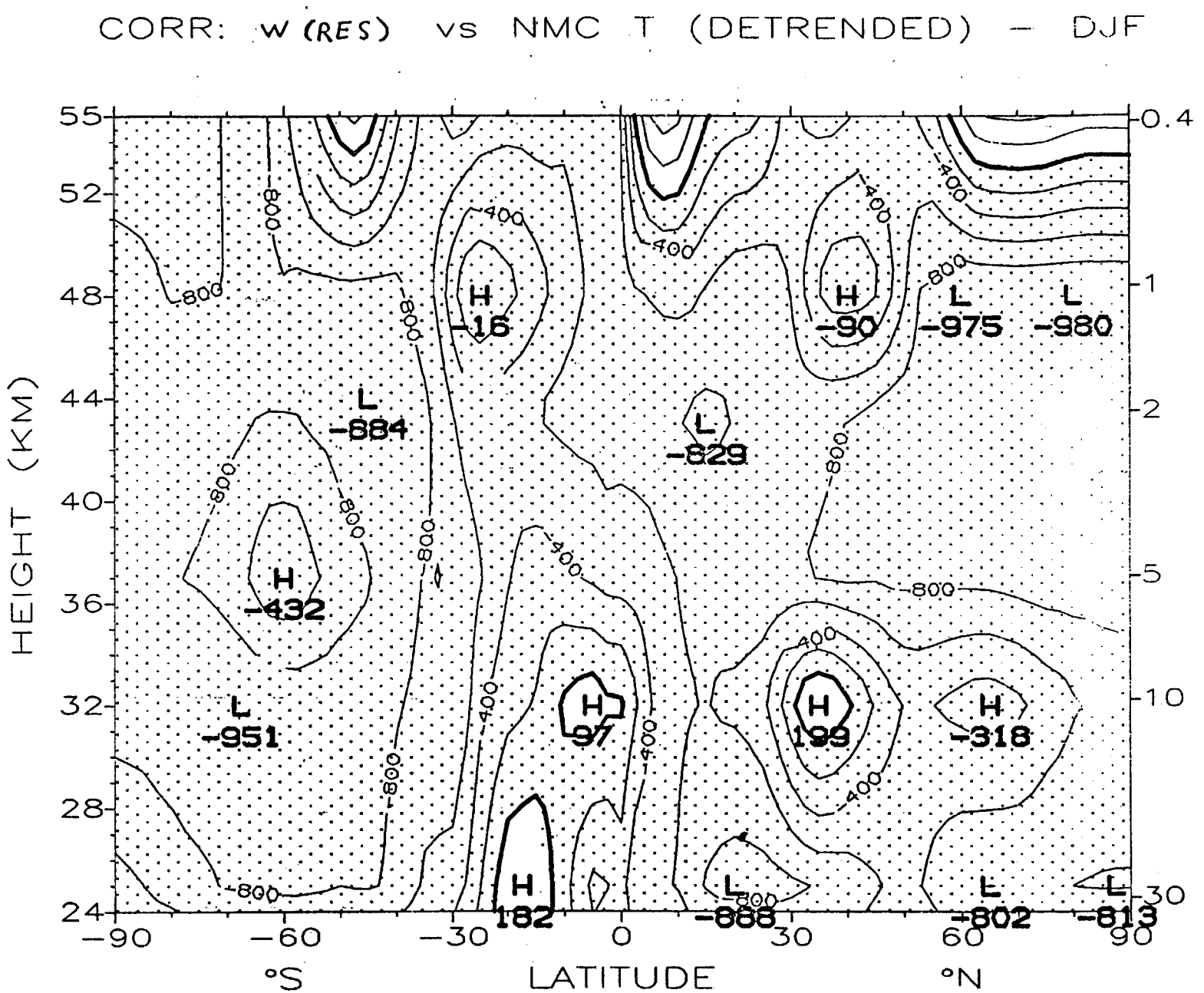
CORR: w (RES) vs NMC T (DETRENDED) – DJF
HEIGHT (KM)
PRESSURE (MB)
55
52
48
44
40
36
32
28
24
0.4
1
2
5
10
30
H -16
H -90
L -975
L -980
L -884
L -829
H -432
L -951
H 97
H 199
H -318
H 182
L -868
L -802
L -813
-800
400
−90
−60
−30
0
30
60
90
°S
LATITUDE
°N
CONTOUR FROM −800.00 TO 400.00 CONTOUR INTERVAL OF 200.00

Figure 5

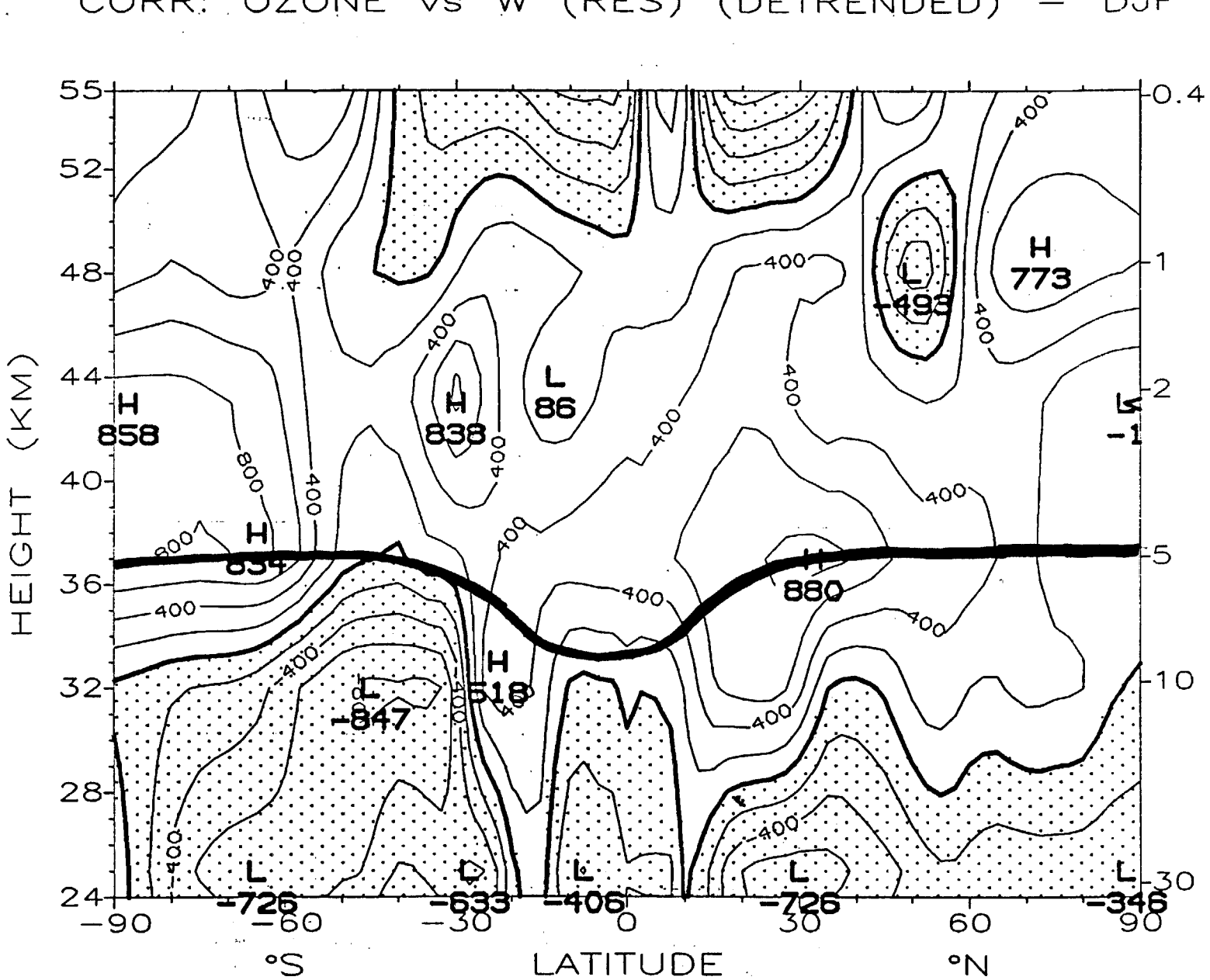
CORR: OZONE vs W (RES) (DETRENDED) — DJF
HEIGHT (KM)
PRESSURE (MB)
55
52
48
44
40
36
32
28
24
0.4
1
2
5
10
30
H 858
H 838
L 86
H 773
L -493
H 880
H 518
L -847
L -726
L -633
L -406
L -726
L -346
400
800
−90
−60
−30
0
30
60
90
°S
LATITUDE
°N
CONTOUR FROM −800.00 TO 800.00 CONTOUR INTERVAL OF 200.00

Figure 6

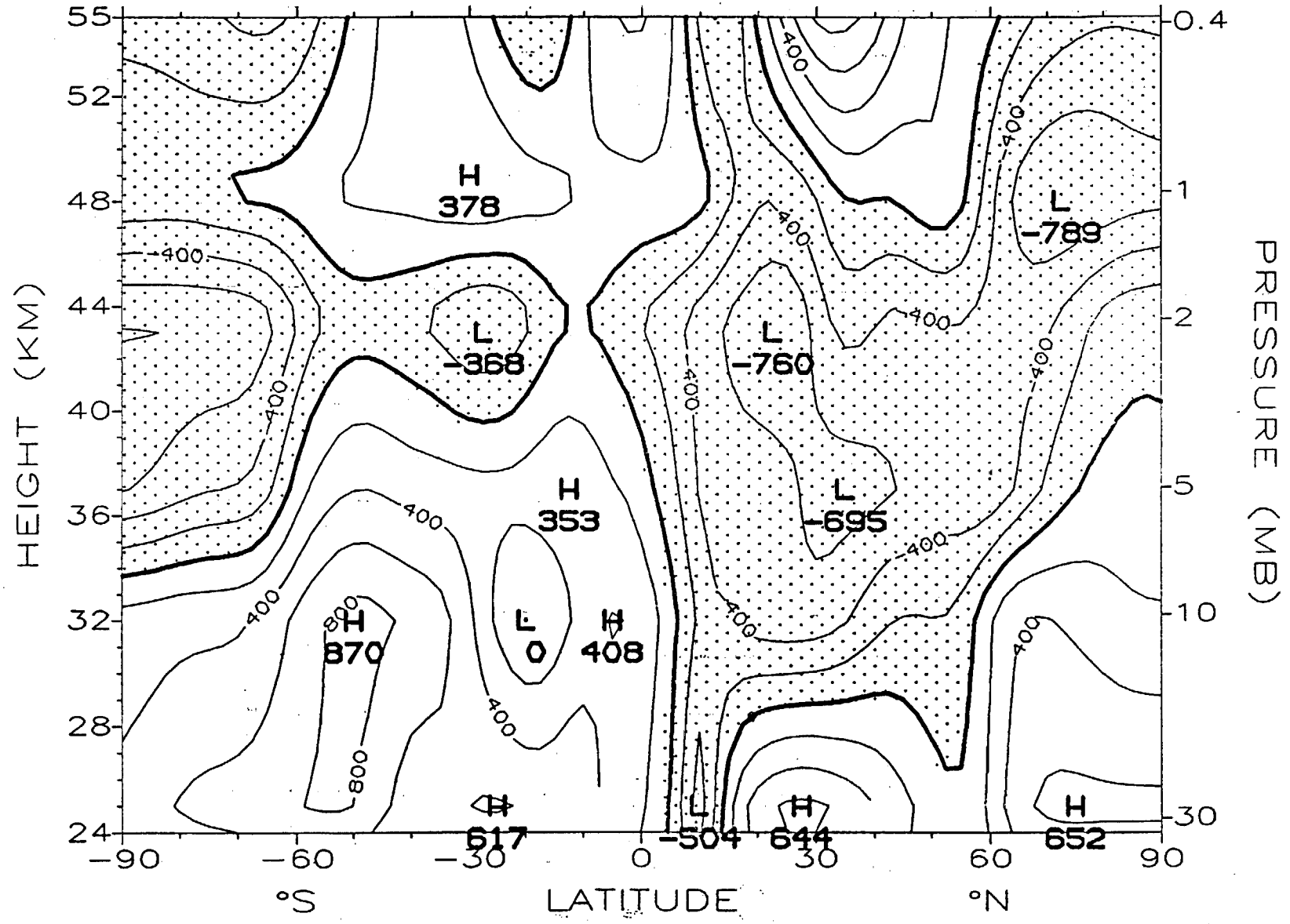
CORR: OZONE vs NMC T (DETRENDED) — DJF
HEIGHT (KM)
PRESSURE (MB)
55
52
48
44
40
36
32
28
24
0.4
1
2
5
10
30
H 378
L -368
L -760
L -789
H 353
L -695
H 870
L 0
H 408
H 617
L -504
H 644
H 652
400
800
-90
-60
-30
0
30
60
90
°S
LATITUDE
°N
CONTOUR FROM -800.00 TO 800.00 CONTOUR INTERVAL OF 200.00

Figure 7

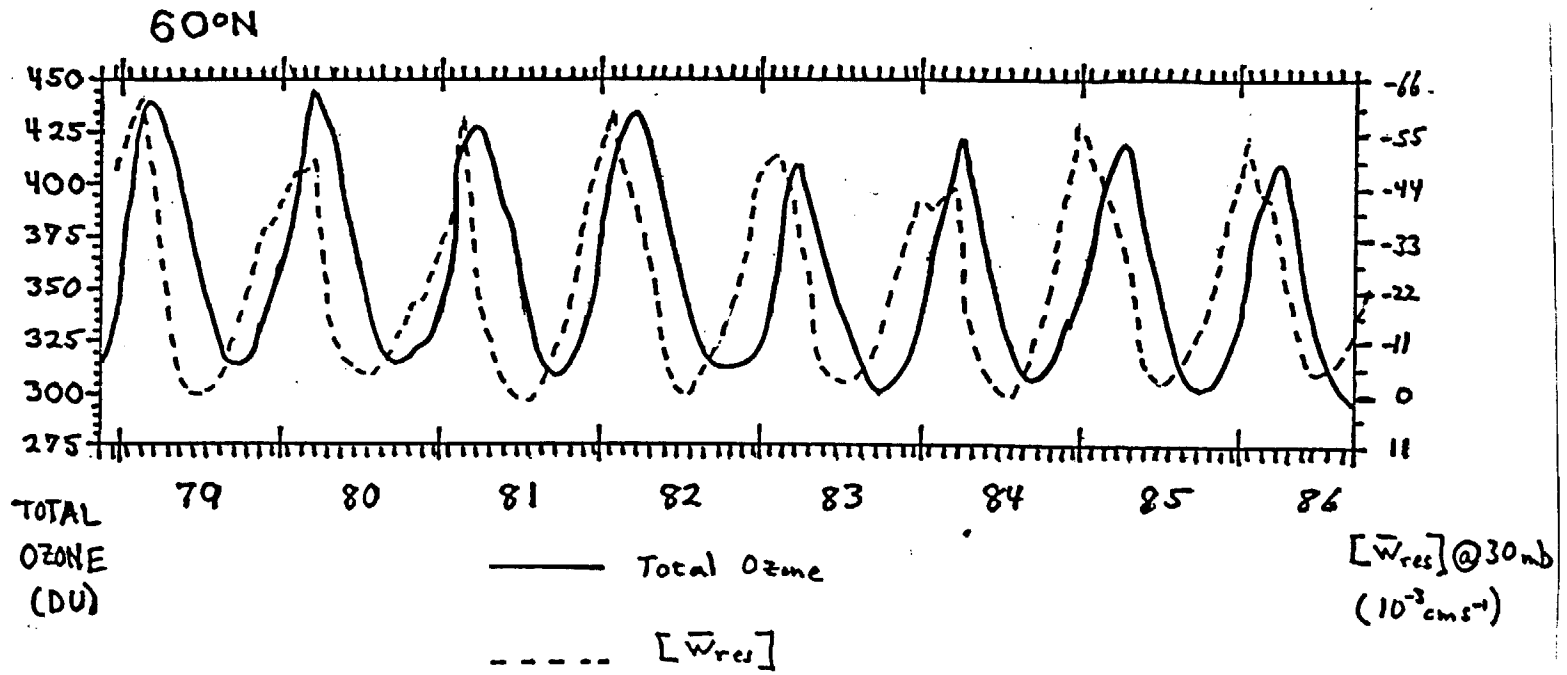
60°N
450
425
400
375
350
325
300
275
-66
-55
-44
-33
-22
-11
0
11
79
80
81
82
83
84
85
86
TOTAL OZONE (DU)
Total Ozone
$[\bar{w}_{res}]$
$[\bar{w}_{res}]$@30mb
(10^{-3} cm s^{-1})

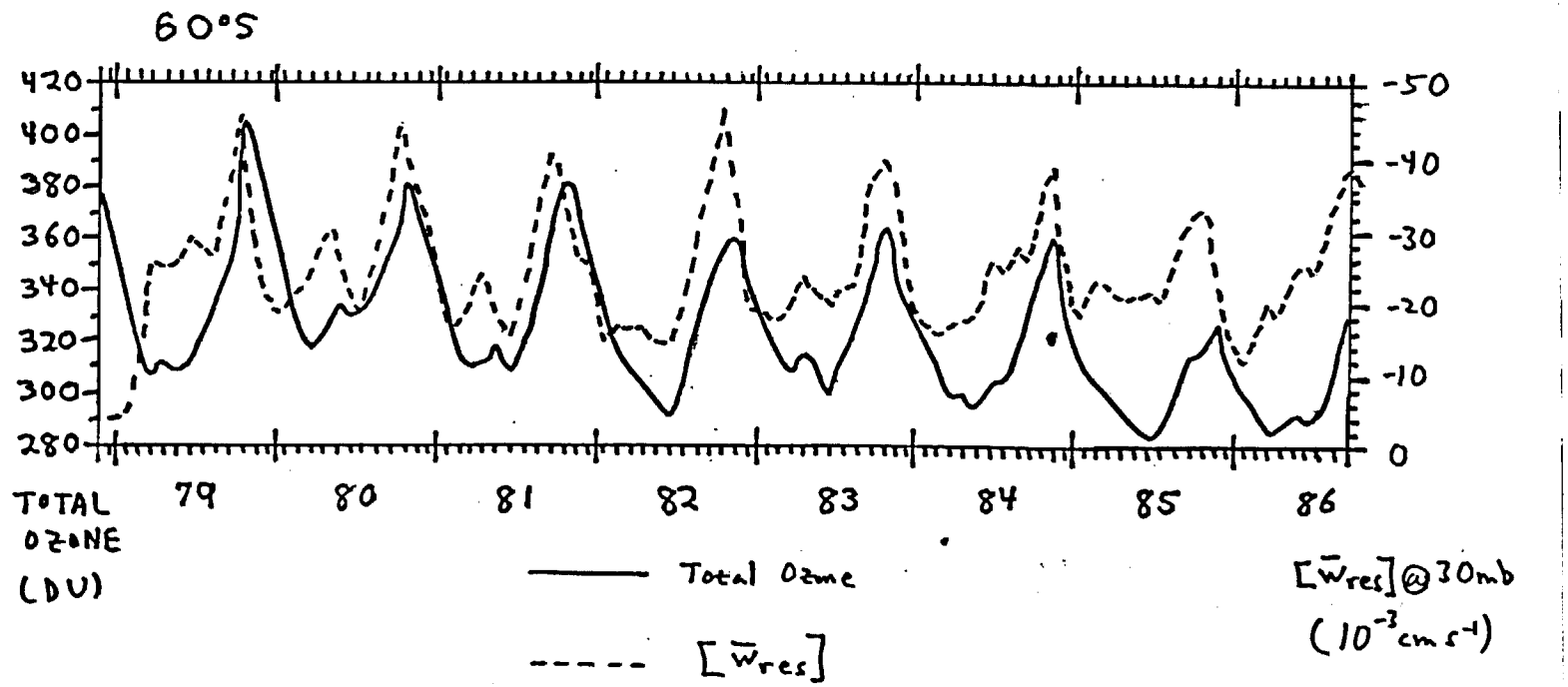
60°S
420
400
380
360
340
320
300
280
-50
-40
-30
-20
-10
0
79
80
81
82
83
84
85
86
TOTAL OZONE (DU)
Total Ozone
$[\bar{w}_{res}]$
$[\bar{w}_{res}]$@30mb
(10^{-3} cm s^{-1})

Figure 8